The Plant Cell, Vol. 18, 3491–3501, December 2006, www.plantcell.org

The Female Gametophyte and the Endosperm Control Cell Proliferation and Differentiation of the Seed Coat in *Arabidopsis* [W]

Mathieu Ingouff, Pauline E. Jullien, and Frédéric Berger[1]

Chromatin and Reproduction Group, Temasek Life Sciences Laboratory, National University of Singapore, Singapore 117604, Republic of Singapore

Double fertilization of the female gametophyte produces the endosperm and the embryo enclosed in the maternal seed coat. Proper seed communication necessitates exchanges of signals between the zygotic and maternal components of the seed. However, the nature of these interactions remains largely unknown. We show that double fertilization of the *Arabidopsis thaliana* female gametophyte rapidly triggers sustained cell proliferation in the seed coat. Cell proliferation and differentiation of the seed coat occur in autonomous seeds produced in the absence of fertilization of the *multicopy suppressor of ira1* (*msi1*) mutant. As *msi1* autonomous seeds mostly contain autonomous endosperm, our results indicate that the developing endosperm is sufficient to enhance cell proliferation and differentiation in the seed coat. We analyze the effect of autonomous proliferation in the *retinoblastoma-related1* (*rbr1*) female gametophyte on seed coat development. In contrast with *msi1*, supernumerary nuclei in *rbr1* female gametophytes originate mainly from the endosperm precursor lineage but do not express an endosperm fate marker. In addition, defects of the *rbr1* female gametophyte also reduce cell proliferation in the ovule integuments before fertilization and prevent further differentiation of the seed coat. Our data suggest that coordinated development of the seed components relies on interactions before fertilization between the female gametophyte and the surrounding maternal ovule integuments and after fertilization between the endosperm and the seed coat.

INTRODUCTION

Organs consist of multiple neighbor tissues containing cells with specific proliferating and differentiating patterns. Precise spatial and temporal regulatory mechanisms must take place to integrate growth (cell division and cell elongation), patterning, and differentiation between the multiple tissues to enable proper organ development.

In flowering plants, a striking example of such complex coordinated control of growth and differentiation occurs during the reproductive phase. In *Arabidopsis thaliana*, sexual reproduction takes place in the haploid female gametophyte embedded within the diploid integuments of the ovule. The female gametophyte (FG) in *Arabidopsis* originates from the surviving haploid meiotic megaspore (stage FG1), which undergoes three successive mitotic divisions (stages FG2, FG3, and FG4) generating a syncytium with eight nuclei (Yadegari and Drews, 2004). At stages FG5 and FG6, cellularization and differentiation take place to generate a seven-cell structure consisting of three antipodals, two synergids, and the two female gametes, the egg cell and the central cell, with one homodiploid nucleus resulting from the fusion of the two haploid polar nuclei (Yadegari and Drews, 2004). After degeneration of the three antipodals (stage FG7), the mature female gametophyte contains the female gametes and the synergids and becomes competent for fertilization (Yadegari and Drews, 2004). Double fertilization consists of the fusion between one sperm cell and the egg cell, resulting in the diploid embryo, and between the second sperm cell and the homodiploid central cell, leading to the development of the triploid endosperm.

In response to fertilization, ovule integuments in *Arabidopsis* differentiate into the seed coat that protects the endosperm and the embryo. Accumulation of tannins (proanthocyanidins [PAs]) is initiated after fertilization in the endothelium of the seed coat (Debeaujon et al., 2003). PA synthesis is controlled by *TRANSPARENT TESTA GLABRA1* (*TTG1*) (Debeaujon et al., 2000) and *TTG2* (Johnson et al., 2002). Loss of function in *TTG2* affects the capacity of seed coat cells to elongate and, in turn, reduces endosperm growth and seed size (Garcia et al., 2005). Hence, the maternal diploid seed coat regulates endosperm growth, which consequently affects the final seed size.

Multiple sources of evidence also demonstrate the role played by the endosperm in the control of cell elongation in the seed coat. The major phase of seed growth parallels the initial endosperm growth characterized by rapid successive rounds of mitoses devoid of cytokinesis (syncytial development) (Garcia et al., 2005). Specific production of diphtheria toxin A in the developing endosperm caused a rapid arrest of seed growth (Weijers et al., 2003). Genetic analyses of the *HAIKU* pathway revealed that reduced syncytial endosperm growth prevents cell elongation in the seed coat, leading to smaller seeds (Garcia

[1] To whom correspondence should be addressed. E-mail fred@tll.org.sg; fax 65-68727007.
The author responsible for distribution of materials integral to the findings presented in this article in accordance with the policy described in the Instructions for Authors (www.plantcell.org) is: Frédéric Berger (fred@tll.org.sg).
[W] Online version contains Web-only data.
www.plantcell.org/cgi/doi/10.1105/tpc.106.047266

et al., 2003, 2005; Luo et al., 2005). The link between endosperm growth and seed coat cell elongation is also supported by parthenogenetic seed development in the *fertilization-independent seed* (*fis*) mutants. This mutant class consists of *medea*, *fis2*, *fertilization independent endosperm* (*fie*), and *multicopy suppressor of ira1* (*msi1*) (Chaudhury et al., 1997; Ohad et al., 1999; Köhler et al., 2003; Guitton et al., 2004). In the absence of fertilization, *fis*-class mutants develop autonomous seeds characterized by an autonomous endosperm developing from the central cell and growth of the seed coat. The parthenogenetic embryo developing in *msi1* autonomous seeds aborts rapidly and thus is unlikely to contribute to cell elongation in the seed coat. *MSI1* and other *FIS* genes encode the four members of the conserved core of the class 2 Polycomb group complex (Grossniklaus et al., 1998; Ohad et al., 1999; Luo et al., 2000; Köhler et al., 2003; Guitton et al., 2004). It was shown that FIE and MIS1 interact with the RETINOBLASTOMA-RELATED homolog RBR1 in *Arabidopsis* (Mosquna et al., 2004) and other plants (Ach et al., 1997). Supporting this interaction, spontaneous nuclear proliferation has been observed in female gametophytes in the absence of fertilization of the *rbr1* mutant in *Arabidopsis* (Ebel et al., 2004). Thus, it has been proposed that RBR1 interacts with the FIS pathway in the control of proliferation of the female gametophyte.

Although cell elongation in the seed coat driven by growth in the endosperm appears to play a major role in the control of seed size, cell proliferation occurs in the seed coat after fertilization (Garcia et al., 2005) and may also play a role in seed size control. Increased cell proliferation in the seed coat causes increased endosperm growth and seed size (Canales et al., 2002; Schruff et al., 2006). However, it is not known whether cell proliferation is regulated in the seed coat in response to fertilization. Besides interactions involving cell proliferation and elongation in the seed coat, evidence has been obtained for interaction between the endosperm and seed coat differentiation in barley (*Hordeum vulgare*) and maize (*Zea mays*) (reviewed in Chaudhury and Berger, 2001), but such evidence is lacking in *Arabidopsis*. One of the steps of integument differentiation in *Arabidopsis* involves the synthesis of flavonoids and is triggered by fertilization (Debeaujon et al., 2003), but the source of the signal involved remains unknown.

Here, we show that rapidly after fertilization, the endosperm triggers sustained cell division in the seed coat. Such active proliferation is also mimicked in the seed coat of autonomous seeds in *msi1* but, surprisingly, not in *rbr1*. Seed coat differentiation is also initiated in *msi1* autonomous seeds but is prevented in the *rbr1* mutant. Further analyses demonstrate that loss of function of *RBR1* alters female gametophyte development and does not generate autonomous seeds. We further observe that defects in the *rbr1* female gametophyte affect cell proliferation in the ovule integuments before fertilization, suggesting a control of the female gametophyte during cell proliferation in the ovule integuments.

RESULTS

Autonomous Development in Emasculated *msi1* and *rbr1* Mutants

To determine further the relative roles played by fertilization signals, the embryo, and the endosperm on seed coat development, we studied autonomously developing seed-like structures produced by the *msi1* and *rbr1* mutants in the absence of fertilization. In the absence of fertilization, the wild-type ovule integuments showed limited growth (Figures 1A and 1B). By contrast, autonomous seed development induced by *msi1* was accompanied by marked integument growth that mimicked to some extent seed coat development in wild-type fertilized seeds (Figures 1C to 1F). Loss of function of *MSI1* has a recessive effect (Köhler et al., 2003) and therefore should not directly affect *msi1*/+ integuments. Seed-like structures produced by *msi1* female gametophytes contain only autonomous endosperm during the first days, when integument growth is observed. We thus hypothesized that *msi1* autonomous endosperm development sustains ovule integument growth, likely reflecting a general role of the endosperm in this process in fertilized seeds.

Overproliferation of nuclei was also observed at the micropylar pole, where the egg cell and synergids differentiate (Ebel et al., 2004). However, we could not find evidence for supernumerary division of the egg or the synergids, although in-depth analysis of egg cell–specific and synergid-specific fate marker expression should be required before a conclusion is drawn. Nuclear proliferation has been reported in *rbr1* female gametophytes, which could lead to the production of seed-like structures containing autonomous endosperm (Ebel et al., 2004). We tested whether loss of function in *RBR1* in the haploid female gametophyte affects integument development several days after emasculation (DAE). Although nuclear proliferation in the *rbr1* female gametophyte could produce up to 20 nuclei by 3 DAE (Figure 1H), the size of the *rbr1* seed-like structures was similar to that of wild-type ovules (cf. Figures 1G and 1H with 1A and 1B, respectively). The lack of response from the integuments could originate from a semidominant action of *rbr1* on ovule integuments, which would make the integuments incompetent to respond to endosperm. This is unlikely, as *rbr1*/+ plants produce wild-type-size seeds from the segregating wild-type gametophytes. Alternatively, the proliferating structure derived from unfertilized *rbr1* gametophytes may not achieve an endosperm identity enabling integument growth. We further analyzed in detail the effect of fertilization and autonomous development in *msi1* and *rbr1* on seed coat development and in parallel analyzed the developmental identity of autonomous proliferating *rbr1* gametophytes.

Analysis of Integument Cell Proliferation

Seed coat growth results from the combination of cell proliferation and cell elongation. The endosperm contributes significantly to seed coat cell elongation at 4 d after pollination (Garcia et al., 2003). However, it was not clear whether endosperm growth could influence cell proliferation in the seed coat earlier than 4 d after pollination. To estimate the effect of fertilization on cell proliferation activity in the seed coat, we quantified the total number of cells per seed, which underwent the transition from the G2-phase to mitosis using the reporter construct $P_{CyclinB1;2}$:glucuronidase ($P_{CycB1;2}$:GUS) (Schnittger et al., 2002). This estimated mitotic activity was compared between the developing seed coat and the integuments of nonfertilized ovules (Figure 2). In the absence of fertilization, ovule integuments showed continuous mitotic activity for 4 DAE with an initial increase around

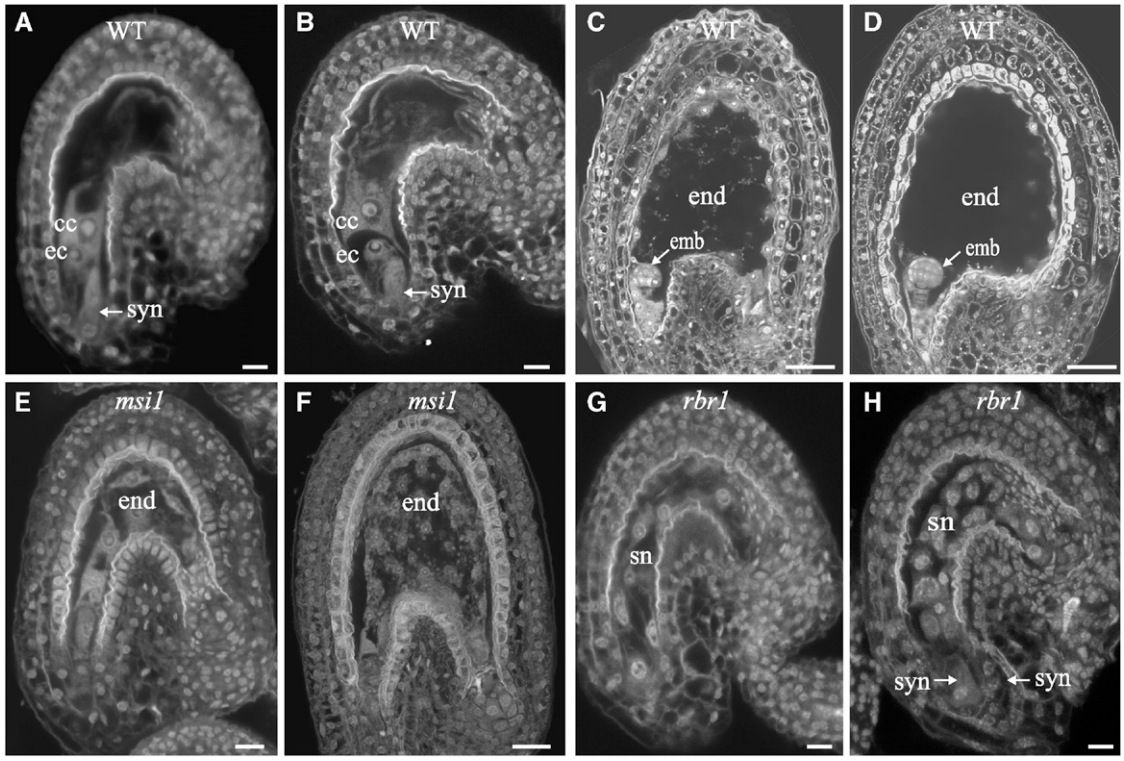

Figure 1. Confocal Sections of *msi1* and *rbr1* Mutant Autonomous Seeds.

Mature flower buds from the wild type (**[A]** and **[B]**) and *msi1* (**[E]** and **[F]**) and *rbr1* (**[G]** and **[H]**) mutants were emasculated and stained with Feulgen at 2 d (**[A]**, **[C]**, and **[E]**) or 3 d (**[B]**, **[D]**, and **[F]**) after emasculation. Emasculated mature flower buds from the wild type were pollinated and stained with Feulgen at 2 d **(C)** or 3 d **(D)** after pollination. In absence of fertilization, the *msi1* mutant forms an autonomous seed that develops a proliferating autonomous endosperm accompanied by seed coat growth (**[E]** and **[F]**; compare with the wild type in **[A]** and **[B]**, respectively). **(E)** represents an example of autonomous endosperm division first observed in a small fraction of the population of ovules. In the *rbr1* mutant (**[G]** and **[H]**), overproliferation of nuclei occurs but is not paralleled by integument growth. cc, central cell; ec, egg cell; emb, embryo; end, endosperm; sn, supernumerary nuclei; syn, synergid. Bars = 25 μm.

ovule maturation and a sharp decline after 2 DAE. A similar trend was observed in the seed coat of developing seeds, with cell proliferation arrest corresponding to the rapid transition to cell elongation in the seed coat at ~4 d after pollination. However, cell proliferation in developing seeds was more intense and sustained compared with that in nonfertilized ovules, suggesting that signals produced by fertilization, the endosperm, and/or the embryo promoted cell proliferation in the seed coat.

To identify the origins of signals stimulating cell proliferation in the seed integuments after fertilization, we introgressed the cell division marker $P_{CycB1;2}$:GUS into *msi1* and *rbr1* mutants and estimated the cell proliferation rate of integuments in the absence of fertilization. We first analyzed *msi1-2*/+; $P_{CycB1;2}$:GUS/$P_{CycB1;2}$:GUS plants. From 3 DAE, two groups of ovules could be distinguished according to their mitotic activity. One of the groups showed higher activity than the wild type and therefore likely resulted from the *msi1* mutation. These ovules showed increased size, as expected for *msi1* autonomous seeds by autonomous endosperm development after 3 DAE. The 1:1 ratio between the two groups indicated a gametophytic genetic segregation of *msi1* (85 wild-type:71 *msi1* ovules analyzed; χ^2 test, $P > 0.26$). Autonomous seeds produced by ovules carrying *msi1* alleles could be distinguished from wild-type unfertilized ovules by increased mitotic activity in the integuments (Figure 2). Compared with wild-type emasculated ovules, seed coat cells of *msi1* autonomous seeds showed a distinctively prolonged phase of cell proliferation. This was parallel to the onset of autonomous proliferation in the endosperm at 1.5 DAE (data not shown). The first division of the parthenogenetic zygote from *msi1* ovules is initiated after 4 DAE (Guitton and Berger, 2005) and thus is unlikely to contribute to the increased mitotic activity in the *msi1* autonomous seed coat, which is observed before 4 DAE. We concluded that autonomous endosperm growth is responsible for the increased mitotic activity in the integuments in *msi1* autonomous seeds. As a similar degree of cell proliferation is eventually achieved in the *msi1* autonomous seed coat and in fertilized seeds, we propose that cell proliferation in the developing seed coat is enhanced by a signal originating from the developing endosperm after fertilization.

In contrast with *msi1*, we did not observe any increased mitotic activity in the integuments of *rbr1* emasculated ovules at 3 DAE. The initial integument cell proliferation in maturing *rbr1* ovules

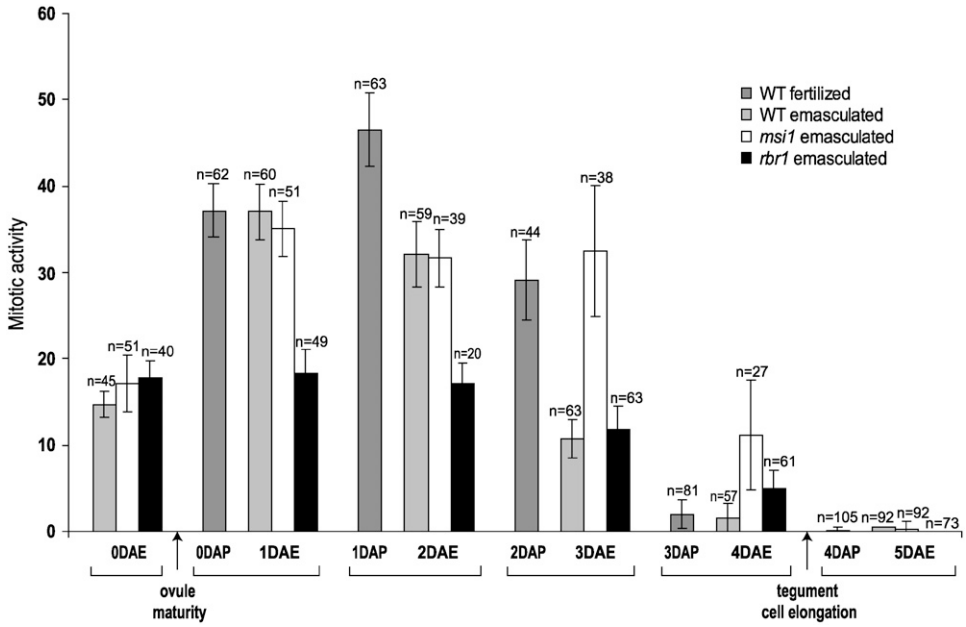

Figure 2. Time-Course Evaluation of Mitotic Activity in the Integument Cells of *msi1* and *rbr1* Autonomous Seeds.

The number of cells expressing the $P_{CycB1;2}$:GUS mitotic marker in the integument cells was estimated from 0 to 5 d after pollination (DAP) for the wild type (dark gray bars) (0 d after pollination corresponds to emasculation time, 12 h before pollination). In parallel, the same experiment was performed on emasculated pistils from 0 to 5 d after emasculation on the wild type (light gray bars), *msi1*/+; $P_{CycB1;2}$:GUS/+ (white bars), and *rbr1*/+; $P_{CycB1;2}$:GUS/+ (black bars). n represents the number of ovules/seeds from which integument cells expressing GUS were counted. Error bars represent SD.

was comparable to that in the wild type (Figure 2). However, *rbr1*/+ plants produced two classes of ovules with either wild-type or reduced mitotic activity that were distinguishable as early as 1 DAE. The relative proportion of each class was compatible with the expected 1:1 segregation ratio for wild-type versus *rbr1* ovules (71 wild-type ovules with cell proliferation and 59 *rbr1* ovules with reduced proliferation; χ^2 test, $P > 0.29$). Although all ovules with a wild-type female gametophyte showed mitotic activity comparable to that in the wild type, most seed-like structures with reduced mitotic activity displayed abnormal female gametophyte development resulting from *RBR1* loss of function. In the *rbr1* mutant, the mitotic activity remained unchanged until 3 DAE (Figure 2). We thus proposed that *rbr1* effects on female gametophyte development limit cell proliferation in the integuments and that supernumerary nuclear divisions in the *rbr1* female gametophyte in the absence of fertilization are not sufficient to trigger a sustained cell proliferation in ovule integuments, as observed in *msi1* autonomous seeds.

Analysis of Seed Coat Differentiation

We further analyzed the differentiation of integument cells in the absence of fertilization in *msi1*/+ and *rbr1*/+ mutants. Fertilization triggers the accumulation of PA pigments in the endothelium cell layer of the seed coat, which can be detected as a red stain by vanillin assay (Debeaujon et al., 2003) (Figure 3B). Wild-type emasculated ovules showed no notable staining at 2 DAE (Figure 3A). By contrast, *msi1* autonomous seeds accumulated PA in the seed coat ($n = 324$) (Figure 3C). Time-course analysis of PA synthesis during autonomous seed development in *msi1* mutants further showed that PA accumulation in *msi1* autonomous seeds closely paralleled the postfertilization differentiation of seed coat cells in wild-type seeds (see Supplemental Figure 1 online). These results suggest that PA accumulation in the endothelium is induced by autonomous *msi1* and wild-type endosperm. However, *msi1* autonomous seeds also contain a parthenogenetic embryo (Guitton and Berger, 2005). Unlike *msi1* autonomous seeds, autonomous seeds from *fis2* solely develop an autonomous endosperm (Guitton et al., 2004). We observed that PA accumulation also occurs in *fis2* autonomous seeds (Figure 3D).

In conclusion, loss of function of *MSI1* triggers the development of autonomous endosperm, which is sufficient to induce increased mitotic activity, PA synthesis, and cell elongation in the seed coat, although fertilization signals and embryo development are absent. We thus propose that endosperm development in wild-type seeds is sufficient for proper seed coat growth and differentiation.

In contrast with *msi1*, *rbr1*/+ integuments surrounding *rbr1* female gametophytes with nuclear proliferation remained unstained after a vanillin assay, as in wild-type emasculated ovules ($n = 422$) (Figure 3E). Excessive nuclear proliferation in the *rbr1* female gametophyte does not trigger the growth and differentiation of a seed coat. Hence, the *rbr1* female gametophyte likely produces a tissue that does not have a proper endosperm identity. Alternatively, the *rbr1* female gametophyte may not reach complete maturity and may retain some proliferative capacity typical of development stages earlier than stage FG5,

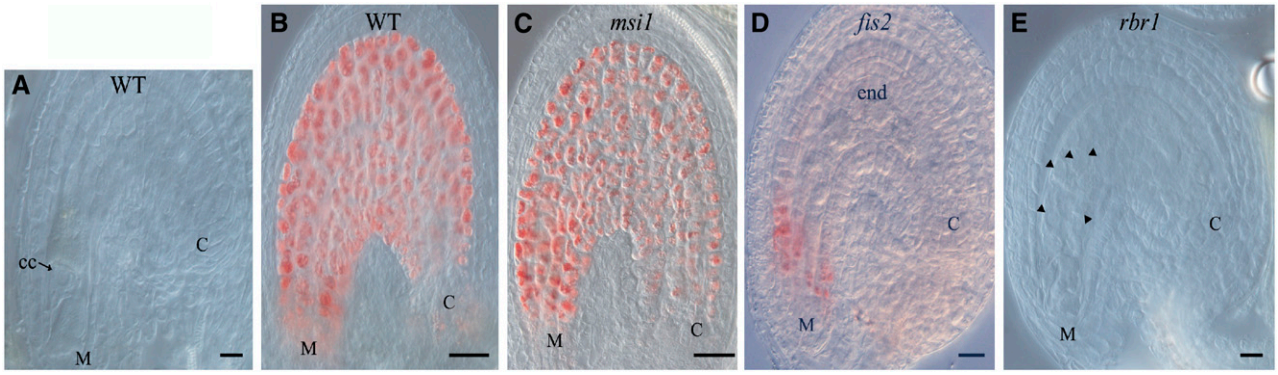

Figure 3. PA Synthesis in *msi1*, *fis2*, and *rbr1* Autonomous Seeds.

PAs are specifically deposited in the endothelium cells of the seed coat upon fertilization. Whole-mount vanillin staining enables direct visualization of PA by staining PA-accumulating cells in red.

(A) Absence of PA in integuments of a wild-type unfertilized ovule.

(B) Uniform detection of PA in the endothelium of a wild-type seed at 3 d after pollination.

(C) Uniform detection of PA in the endothelium of an *msi1* autonomous seed at 3 DAE.

(D) Accumulation of PA in the endothelium of a *fis2* autonomous seed at 2 DAE.

(E) Absence of PA in integument cells of an *rbr1* autonomous seed at 2 DAE.

Arrowheads indicate supernumerary nuclei typical of the *rbr1* mutant. C, chalazal pole; cc, central cell; end, endosperm; M, micropylar pole. Bars = 25 μm.

when cellularization is initiated and fusion of the polar nuclei forms the central cell (Yadegari and Drews, 2004).

Developmental Identity of the *rbr1* Proliferating Gametophyte

To determine cell fate in syncytial proliferating *rbr1* female gametophytes, we analyzed the expression of the endosperm-specific marker KS117 in the *rbr1*/+ genetic background. KS117 is not detected in the wild-type female gametophyte but is expressed after fertilization in the endosperm as early as stage IV/V (8/16 nuclei) (Ingouff et al., 2005). KS117 is expressed during *msi1* autonomous seed development (Guitton and Berger, 2005). At 3 DAE, supernumerary nuclei in *rbr1* female gametophytes did not exhibit any expression of KS117 ($n = 252$). This absence of endosperm marker expression showed that the *rbr1* female gametophyte does not develop an endosperm-like structure, suggesting that overproliferating tissues in *rbr1* ovules retain a gametophytic identity in the absence of fertilization.

We analyzed the expression of P_{MYB98}:green fluorescent protein (P_{MYB98}:GFP), a marker of female gametophyte maturation (Kasahara et al., 2005), during *rbr1* female gametophyte development. At stage FG5, when the migration of polar nuclei occurs to form the central cell (Drews and Yadegari, 2002), P_{MYB98}:GFP was expressed uniformly in the wild-type female gametophyte except in the antipodals at the chalazal pole (Figure 4A) (Kasahara et al., 2005). At maturity (stage FG7), P_{MYB98}:GFP expression became restricted mainly to the two synergids, but a weak expression remained in the egg cell and the central cell (Figure 4B). After fertilization, P_{MYB98}:GFP persisted in the intact synergid and was detected in the endosperm (Figure 4C). In *rbr1* female gametophytes, P_{MYB98}:GFP was expressed at very high levels in synergids, suggesting that synergid identity was not perturbed by *rbr1*. However, P_{MYB98}:GFP expression was never restricted to the synergids, as in wild-type mature female gametophytes, and it persisted in the chalazal part of the female gametophyte showing nuclear overproliferation (Figure 4D). As *rbr1* female gametophyte proliferating tissue did not assume an endosperm identity, the unrestricted MYB98 expression suggests that an abnormal gametophytic identity persists in overproliferating *rbr1* female gametophytes. Supernumerary nuclei in the proliferating *rbr1* gametophytic tissue expressed P_{MEDEA}:GUS (Figure 5C), a marker of the central cell lineage detected from stage FG5 specifically in polar nuclei (Figure 5A) and after the fusion of polar nuclei in the central cell (stage FG6) (Figure 5B) (Luo et al., 2000). This finding suggested that supernumerary nuclei in *rbr1* female gametophytes derive mainly from unrestricted proliferation of the central cell lineage. This result was supported by the absence of obvious proliferation of cells from the egg apparatus, which contained two synergids and a single egg cell, as in wild-type female gametophytes (see Supplemental Figure 2 online). We further analyzed the mitotic activity of the various cells of the *rbr1* female gametophyte in *rbr1*/+; $P_{CycB1;2}$:GUS/+ plants. After emasculation, we could not detect any GUS activity in ovules from wild-type pistils (Figure 6A; $n = 435$). By contrast, GUS staining was observed at low frequency in a low percentage of *rbr1* female gametophytes at 3 DAE (five positive ovules; $n = 816$). In all of these cases, GUS activity was detected only around nuclei derived from the central cell and not from the egg apparatus (Figure 6B; $n = 5$). This shows that extra nuclei in *rbr1* female gametophyte derive mostly from the proliferation of the central cell lineage.

To further understand the origin of the defects of *rbr1* female gametophytes, we established the expression pattern of RBR1 during female gametophyte development. The whole *RBR1*

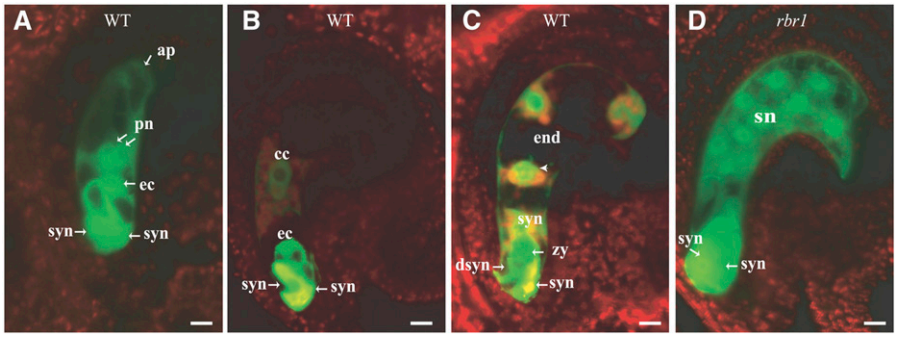

Figure 4. Expression of the P_{MYB98}:GFP Marker in a Female Gametophyte of the *rbr1* Mutant.

(A) to **(C)** Wild type. Expression pattern of the P_{MYB98}:GFP marker in the female gametophyte.
(A) P_{MYB98}:GFP is detected in all parts of the female gametophyte before fusion of the polar nuclei (stage FG5), except in antipodals.
(B) Later, GFP is restricted mainly to the synergids, but a weak signal remains in the egg cell and the central cell (stage FG7).
(C) After fertilization, expression is detected in the intact synergid and in the endosperm at the four-nuclei stage.
(D) *rbr1* mutant. Expression is never restricted to the synergids and remains in all parts of the *rbr1* female gametophyte. The highest signal intensity is still detected in the synergids, as in the wild type.
ap, antipodals; cc, central cell; dsyn, degenerate synergid; ec, egg cell; end, endosperm; pn, polar nuclei; sn, supernumerary nuclei; syn, synergid; zy, zygote. Bars = 10 μm for **(A)** and 25 μm for **(B)** to **(D)**.

locus containing the promoter and the downstream sequences was fused in frame with the monomeric Red Fluorescent Protein1 (mRFP1) (Campbell et al., 2002). The P_{RBR1}:RBR1-mRFP1 translational fusion construct was transformed into selected *rbr1-2* mutant plants. Expression of the RBR1-mRFP1 fusion rescued the *rbr1-2* mutation, hence demonstrating functionality (see Supplemental Figure 3 online). The dynamic localization of RBR1-mRFP1 was then studied by confocal microscopy during female gametophyte development (Figure 7). The fusion protein RBR1-mRFP1 showed a salt-and-pepper distribution in the ovule integument cells, as observed previously for *RBR1* mRNAs in root meristems (Wildwater et al., 2005). This probably reflects the control of *RBR1* expression by the cell cycle machinery. In the female gametophyte, the RBR1-mRFP1 fusion protein was detected mostly in nuclei (Figure 7). At stage FG1, RBR1-mRFP1 was present in the nucleus of the surviving megaspore mother cell (Figure 7A). RBR1-mRFP1 expression persisted in all nuclei during the three synchronous mitoses leading to stages FG2/3 (Figure 7B), FG4 (Figure 7C), and FG5 (Figure 7D). During stage FG5, the overall expression of RBR1-mRFP1 decreased, and after polar nuclei fusion (stage FG6), RBR1-mRFP1 persisted mostly in the central cell of the female gametophyte (Figure 7E). At maturity, RBR1-mRFP1 was completely excluded from the egg apparatus and was expressed only in the central cell (stage FG7; Figure 7F). The restricted expression of RBR1 to the central cell at ovule maturity supports the notion that cell cycle arrest in this cell depends directly on RBR1 function. In conclusion, we propose that *rbr1* female gametophytes proceed normally

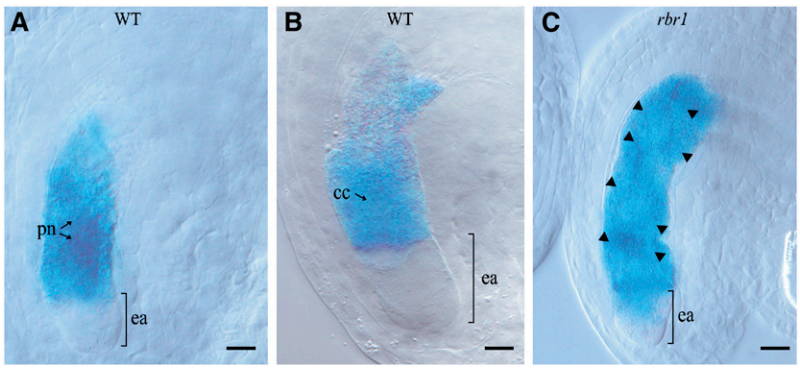

Figure 5. Expression of the P_{MEDEA}:GUS Marker in a Female Gametophyte of the *rbr1* Mutant.

(A) and **(B)** Wild type. P_{MEDEA}:GUS staining in the female gametophyte was described previously by Luo et al. (2000). GUS activity is detected in the polar nuclei **(A)** and in the central cell upon fusion of the polar nuclei **(B)**.
(C) *rbr1* mutant. GUS staining is detected in supernumerary nuclei (arrowheads) in the *rbr1* female gametophyte.
cc, central cell; ea, egg apparatus; pn, polar nuclei. Bars = 10 μm.

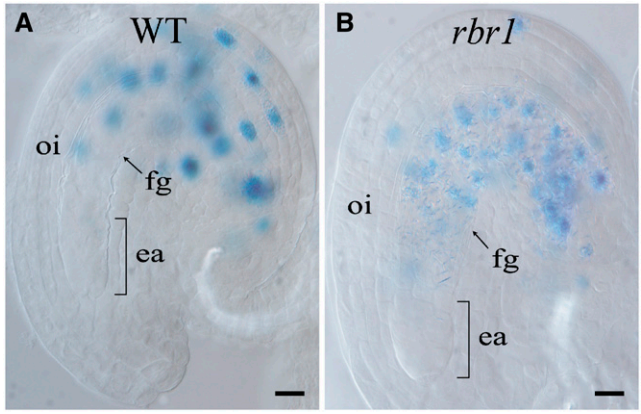

Figure 6. Expression of the Mitotic Marker $P_{CycB1;2}$:GUS in a Female Gametophyte of the *rbr1* Mutant.

(A) Wild type. Salt-and-pepper GUS staining pattern in a cleared ovule.
(B) *rbr1* mutant. Marked GUS expression in the supernumerary nuclei in the chalazal and central regions of the female gametophyte. No GUS activity is detected in the egg apparatus.
ea, egg apparatus; fg, female gametophyte; oi, ovule integuments. Bars = 10 μm.

through the three successive mitoses (stages FG1 to FG4) but fail to arrest nuclear division after the third mitosis, when cellularization occurs and differentiation is initiated (Christensen et al., 1997). Our cellular and marker gene expression analyses indicate that the *rbr1* female gametophyte differentiation is initiated but might not be complete.

DISCUSSION

Fertilization Enhances Cell Proliferation and Triggers Differentiation of the Seed Coat

Our study on cell proliferation in the seed coat shows that a sustained mitotic activity is triggered after fertilization and persists until 3 d after pollination. In response to fertilization, the differentiation of ovule integuments into seed integuments is activated (Haughn and Chaudhury, 2005) with the accumulation of PAs in the endothelium (Debeaujon et al., 2003) and cell elongation (Garcia et al., 2005).

We showed that *msi1* autonomous endosperm development triggers cell proliferation, cell elongation, and differentiation of the seed coat. Although a nonviable parthenogenetic embryo also develops in *msi1* autonomous seeds, *msi1* autonomous seed development results mainly from autonomous endosperm growth (Guitton and Berger, 2005). Autonomous seed development in *fis2* involves only autonomous endosperm development (Guitton et al., 2004), which appears to be sufficient to trigger PA synthesis. No significant growth of the seed coat is observed in seeds in which only the egg cell is fertilized as a result of the production of a single sperm cell in A-type *cyclin-dependent kinase1* mutant pollen (Nowack et al., 2006). Similarly, ablation of endosperm in developing seeds results in extremely reduced seed coat development (Weijers et al., 2003). Thus, we propose that fertilization of the egg cell and consequent embryo development may not play a major role in seed coat growth. We propose that activation of the central cell and consequent endosperm development are probably the key players in the transition from ovule integument proliferation to seed coat

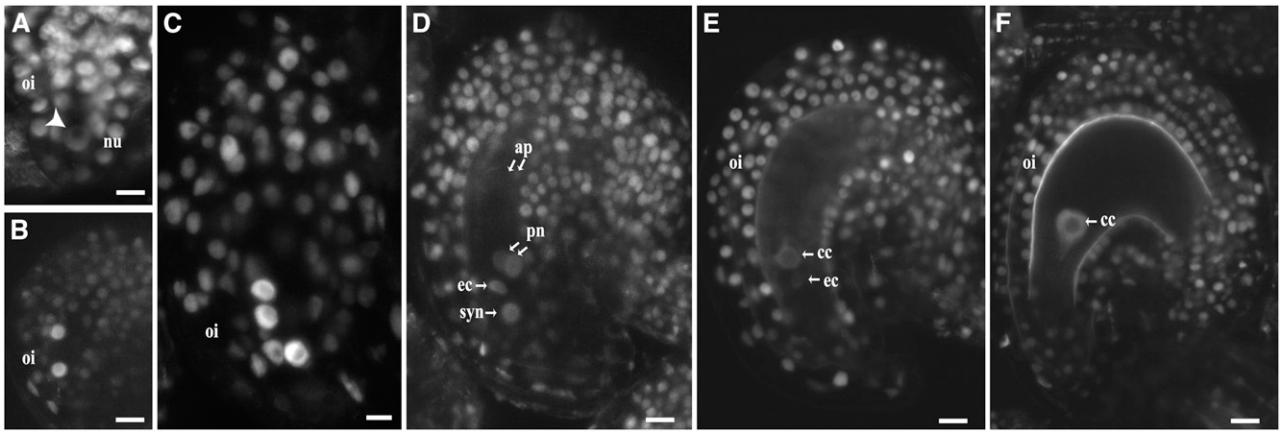

Figure 7. Dynamic Analysis of the P_{RBR1}:RBR1-mRFP1 Fusion Protein during Female Gametophyte Development.

Confocal images from the RBR1-mRFP1 fusion protein under the control of its native promoter were obtained from 11 independent stable transformed plants.
(A) Ovule with the megaspore (arrowhead).
(B) Two-nucleate-stage ovule.
(C) Four-nucleate-stage ovule.
(D) Eight-nucleate-stage ovule.
(E) Maturing female gametophyte.
(F) Mature female gametophyte.
ap, antipodals; cc, central cell; ec, egg cell; nu, nucellus; oi, ovule integuments; syn, synergid. Bars = 5 μm for **(A)** and 10 μm for **(B)** to **(F)**.

growth and differentiation in the wild-type seed. The signals originating from the maturing female gametophyte and developing endosperm, involved in ovule integument and the seed coat, respectively, remain to be identified.

The *rbr1* Mutation Does Not Trigger Autonomous Seed Development

In absence of fertilization, *fis*-class mutants, including *mea*, *fis2*, *fie*, and *msi1*, develop an autonomous endosperm from the unfertilized central cell accompanied by autonomous seed development and parthenocarpy (Köhler et al., 2003; Guitton et al., 2004). This common phenotype is supported by the ability of the three FIS Polycomb group proteins together with MSI1 to assemble in a complex (Köhler et al., 2003; Bracha-Drori et al., 2004; Chanvivattana et al., 2004).

MSI1 and RBR1 homologs are able to bind to each other (Ach et al., 1997) and may form complexes with the Polycomb group partner FIE (Mosquna et al., 2004). Based on the biochemical data and the presence of overproliferating nuclei in *rbr1* female gametophytes, it was reasonably proposed that this mutant phenotype was reminiscent of an autonomously developing endosperm typical of the *fis* Polycomb group mutant (Ebel et al., 2004). However, our study indicates that *rbr1* ovules are unable to express an early endosperm marker and to induce endosperm-derived signals necessary for the differentiation of seed coat cells. Rather, although sustained nuclear proliferation is observed in the female gametophyte, *rbr1* ovules degenerate in the absence of fertilization similarly to the wild type.

In conclusion, overproliferation of nuclei from *rbr1* female gametophytes does not reflect autonomous endosperm development, and the *rbr1* mutant is unable to promote an autonomous seed developmental program.

During the three successive mitoses of female gametophyte development (stages FG1 to FG5), RBR1 is expressed in all nuclei of the female gametophyte to become restricted to the female gametes (stage FG6). Eventually, RBR1 becomes confined to the central cell and excluded from the egg cell in the mature female gametophyte (stage FG7). This suggests that cell cycle arrest is different in the two female gametes, the central cell and the egg cell. Retinoblastoma proteins in mammals and plants are central cell cycle regulators that prevent cell division by blocking the transition from G1- to S-phase in the cell cycle (Inze, 2005). The restriction of RBR1 protein to the central cell in the mature female gametophyte suggests that this cell is arrested in G1-phase.

Confinement of RBR1 to the central cell further suggests that supernumerary nuclei in *rbr1* mature female gametophytes originate from the central cell lineage and not from the egg apparatus lineage, as reported previously (Ebel et al., 2004). This is consistent with the expression of a marker of the central cell lineage in the chalazal pole of *rbr1* female gametophytes and of the mitotic cyclin B1,2 reporter. Our microscopic analyses further suggest that the integrity of the egg apparatus is preserved in *rbr1* ovules, which progress through the initial stages of gametophytic divisions. Excessive proliferation from the micropylar pole observed in previous studies (Ebel et al., 2004) may originate from a smaller fraction of *rbr1* gametophytes affected by early arrest or by abnormal precocious cellular development. Additional specific markers for antipodals and the egg cell will be necessary to precisely establish cell fate identity in all classes of *rbr1* female gametophytes.

The Female Gametophyte Controls Cell Proliferation in Ovule Integuments

Before fertilization, ovule growth implies coordinated growth between the enlarging female gametophyte and the surrounding inner and outer integuments. Our results show that integument cell proliferation intensity is sustained as ovules reach maturity (Figure 2). This marked mitotic activity upon terminal ovule maturation is absent in *rbr1* ovule integuments (Figure 2). This finding suggests that the perturbed proliferation rate in *rbr1*/+ integument cells results from defects in haploid female gametophytes. Our analyses of markers of the female gametophyte in the *rbr1* mutant background suggest that *rbr1* female gametophytes are affected when differentiation is initiated by stage FG5. We propose that final steps of female gametophyte maturation promote integument cell proliferation to enable terminal growth of the female gametophyte before fertilization. This suggests that the maturing female gametophyte conveys cell proliferation–promoting signals to the surrounding ovule integuments. However, the importance of such signals is likely to be only moderate, as integuments develop to some extent in *spl* mutant ovules, which do not contain embryo sacs (Schiefthaler et al., 1999; Yang et al., 1999).

It is unknown whether signals originating from surrounding ovule integuments toward the female gametophyte also exist. However, mutations affecting the initiation and development of the ovule integuments often lead to an absence or an early block of female gametophyte development, suggesting that proper ontogenesis of the female gametophyte also involves signals from the surrounding inner integument (Reiser et al., 1995; Elliot et al., 1996; Klucher et al., 1996; Baker et al., 1997; Schneitz et al., 1997).

In conclusion, reciprocal controls likely take place between the female gametophyte and its surrounding integuments before and after fertilization to integrate the multiple parameters necessary to ensure the coordination of sporophytic and gametophyte programs and successful transmission of the offspring.

METHODS

Plant Strains and Growth Conditions

The *Arabidopsis thaliana rbr1* mutant alleles (Columbia accession) used in this study were *rbr1-1* (SALK_012270; SALK collection), *rbr1-2* (SALK_002946; SALK collection), and *rbr1-3* (GABI_170G02; GABI-Kat collection) (Ebel et al., 2004). The *msi1* mutant alleles were *msi1-1* (Columbia accession) (Köhler et al., 2003) and *msi1-2* (C24 accession) (Guitton et al., 2004). The *fis2* mutant allele (*fem17*; Columbia accession) was provided by Gary Drews (Christensen et al., 1997).

The enhancer trap mGFP5 line KS117 (C24 accession) was identified after a screen in Jim Haseloff's collection (Haseloff, 1999; Ingouff et al., 2005). The transgenic line containing the construct P_{MEDEA}:GUS reporter line (C24 accession) was provided by Abed Chaudhury (Luo et al., 2000). The transgenic seeds (Columbia accession) for the construct P_{MYB98}:GFP

were a gift from Gary Drews (Kasahara et al., 2005). The marker line (Landsberg *erecta* accession) containing the construct $P_{CycB1;2}$:GUS was given by Arp Schnittger (Schnittger et al., 2002).

After 2 d of stratification at 4°C in the dark, seeds were germinated and grown on soil. Plants were cultured in a growth chamber under short days (8 h of light at 20°C/16 h of dark at 16°C; 60 to 70% RH) until rosettes were formed. Seedlings were transferred to long days at 20°C (14-h day/10-h night) to induce flowering and grown until seeds were harvested.

Microscopy

GUS assay was performed as reported previously (Boisnard-Lorig et al., 2001). After an overnight incubation at 37°C, stained developing pistils were dissected and ovules or seeds were cleared with a derivative of Hoyer's medium and observed microscopically with differential interference contrast optics (DM6000 B; Leica). Images were acquired with a DXM1200F digital camera (Nikon) and processed with Metamorph (version 6.2; Universal Imaging).

Fluorescence was imaged using laser scanning confocal microscopy (Zeiss LSM-510) for GFP with selective settings for GFP detection (excitation, 488 nm; emission, band-pass 510 to 550 nm) and nonspecific settings for autofluorescence detection (excitation, 543 nm; emission, long-pass 560 nm) and for mRPF1 (excitation, 543 nm; emission, band-pass 560 to 615 nm).

Image acquisition on fixed tissues was performed on a Zeiss LSM-510 laser scanning confocal microscope using the 488-nm excitation line of an argon laser and a long-pass emission filter at 510 nm. Digital image processing was performed with Adobe Photoshop and Adobe Illustrator (Adobe Systems).

Time-Course Evaluation of Mitotic Activity in the Integuments

The total number of cells at the G2/M transition was counted per ovule integument and per seed coat using the marker of mitotic activity, $P_{CycB1;2}$:GUS. Analyses of cell division activity were performed on segregating wild type and *rbr1-3* and *msi1-2* mutants homozygous for $P_{CycB1;2}$:GUS. Flowers at 1.5 d before anthesis were emasculated each day for 5 d to estimate integument cell proliferation. In parallel, emasculated pistils from wild-type plants at 1.5 d before anthesis were pollinated 24 h later with pollen from homozygous $P_{CycB1;2}$:GUS plants. Samples were collected and stained for GUS. Measurement of any integument cell with GUS expression was obtained for individual ovules taken at random. In populations of ovules from *msi1-1*/+ plants, before 2 DAE, all ovules showed similar mitotic activity. After 3 DAE, two groups of ovules became distinguishable. Ovules from one group had mitotic activity similar to emasculated wild-type ovules, whereas ovules from the other group showed higher mitotic activity and were presumably *msi1-1* mutant ovules. The average value considered for the graph was the mean from the latter group. Similarly, ovules from emasculated *rbr1-3*/+ plants segregated into two groups after 1 DAE. For consideration in the graph, the group with lower activity than the wild type was chosen.

Analysis of the Phenotype Conferred by *rbr1*

Pistils from *rbr1-2* and *msi1-1* mutants were emasculated 1 d before anthesis and collected 2 or 3 d later. Pistils were cut at the tip, stained with Schiff's reagent (Sigma-Aldrich), and embedded in LR White (Sigma-Aldrich) according to Braselton et al. (1996). The mutant lines *rbr1-2* and *msi1-1* can only be propagated as heterozygotes and produce pistils that contain 50% wild-type ovules and 50% ovules that display the mutant phenotype.

The P_{MEDEA}:GUS and P_{MYB98}:GFP reporter gene constructs and the KS117 endosperm marker were introgressed respectively into *rbr1-1* and *rbr1-2* by crossing. Analyses were performed on *rbr1* mutants homozygous for the marker. At 2 DAE, pistils from *rbr1-2*; KS117/KS117 were dissected to determine GFP activity. Emasculated pistils from *rbr1-1*; P_{MEDEA}:GUS/P_{MEDEA}:GUS and *rbr1-1*; P_{MYB98}:GFP/P_{MYB98}:GFP were analyzed at 1 DAE.

Whole-Mount Staining for Detection of PAs

Emasculated pistils at 1.5 d before anthesis from *rbr1-2*/+ and *msi1-1*/+ mutants were left unpollinated for 3 d to promote autonomous seed development. Emasculated pistils at 1.5 d before anthesis from the wild type were pollinated at 1.5 d after emasculation to be used as a reference.

For the time-course analysis of PA synthesis during autonomous seed development in *msi1-1*, 10 pistils at 1.5 d before anthesis were emasculated every day for 3 d.

Ovules and seeds were dissected from pistils and siliques, respectively, and incubated in an acidic solution (6 N HCl) of 1% (w/v) vanillin (Sigma-Aldrich) at room temperature (Aastrup et al., 1984). Vanillin reacts in the presence of PAs that specifically accumulate in the endothelium layer of the seed coat, generating a red product (Debeaujon et al., 2003). Microscopic observations were performed with differential interference contrast optics (DM6000 B; Leica). Images were acquired with a DXM1200F digital camera (Nikon) and processed with Metamorph (version 6.2; Universal Imaging).

RBR1:RBR1-mRFP1 Plasmid Construction and Transformation

A 6968-bp fragment of *RBR1* containing 2 kb upstream of the ATG until the last codon before the termination codon of the gene was amplified by PCR with the KOD-plus-PCR kit (Toyobo) and cloned directionally between the Gateway *att*L recombination sites of the plasmid pENTR-D-TOPO (Invitrogen) to generate the pENTR-D-TOPO-P_{RBR1}:RBR1 entry vector.

The fragment containing the cassette Gateway *att*R, mRFP1, and the nopaline synthase (NOS) terminator (K7GW-mRFP1-NOS) was cloned into the binary plasmid pALLIGATOR2 (Bensmihen et al., 2004; http://www.isv.cnrs-gif.fr/jg/alligator/vectors.html) to generate pAlli2-K7GW-mRFP1-NOS.

Recombination reactions (*att*L × *att*R) were performed between the destination vector pAlli2-K7GW-mRFP1-NOS and the pENTR-D-TOPO-P_{RBR1}:RBR1 entry vector to produce the vector pAlli2-P_{RBR1}:RBR1-mRFP1-NOS.

rbr1-2/+ mutant (kanamycin-selected) plants were transformed using the *Agrobacterium tumefaciens*–mediated floral dip method (Clough and Bent, 1998). The pALLIGATOR vectors contain the *GFP* gene driven by a seed storage protein promoter, At2S3, enabling direct visual selection. Primary seed transformants were collected based on their fluorescence level in the seed and further selected on Murashige and Skoog plates supplemented with kanamycin (50 mg/L). Eleven transgenic lines were obtained, all showing a similar pattern of expression. Complementation was achieved by transformation of *rbr1-2*/+ plants with the *RBR1* locus fused to *mRFP1*. Complementation was analyzed on one line.

Accession Numbers

Accession numbers for the *MSI1* and *RBR1* genes are At5g58230 and At3g12280, respectively.

Supplemental Data

The following materials are available in the online version of this article.

Supplemental Figure 1. Time-Course Analysis of PA Synthesis during Autonomous Seed Development in the *msi1* Mutant.

Supplemental Figure 2. Frontal View of the *rbr1* Female Gametophyte.

Supplemental Figure 3. Complementation of the *rbr1-2* Mutant with the *RBR1* Locus Fused to *mRFP1*.

ACKNOWLEDGMENTS

We thank Lars Henning for providing the *msi1-1* allele, Arp Schnittger for his gift of the marker $P_{CycB1;2}$:GUS, Abed Chaudhury for the marker P_{MEDEA}:GUS, and Gary Drews for the marker P_{MYB98}:GFP. We thank the ABRC for providing us with the *rbr1-1* and *rbr1-2* mutant alleles and GABI-Kat for the *rbr1-3* mutant allele. We are grateful to Francois Parcy for providing us with the Alligator plasmids. P.E.J. and F.B. were supported by the Temasek Lifesciences Laboratory and by the National University of Singapore. M.I. was supported by the Singapore Millennium Foundation.

Received September 8, 2006; revised October 27, 2006; accepted November 7, 2006; published December 15, 2006.

REFERENCES

Aastrup, S., Outtrup, H., and Erdal, K. (1984). Location of the proanthocyanidins in the barley grain. Carlsberg Res. Commun. **49,** 105–109.

Ach, R., Taranto, P., and Gruissem, W. (1997). A conserved family of WD-40 proteins binds to the retinoblastoma protein in both plants and animals. Plant Cell **9,** 1595–1606.

Baker, S.C., Robinson-Beers, K., Villanueva, J.M., Gaiser, J.C., and Gasser, C.S. (1997). Interactions among genes regulating ovule development in *Arabidopsis thaliana*. Genetics **145,** 1109–1124.

Bensmihen, S., To, A., Lambert, G., Kroj, T., Giraudat, J., and Parcy, F. (2004). Analysis of an activated *ABI5* allele using a new selection method for transgenic *Arabidopsis* seeds. FEBS Lett. **12,** 127–131.

Boisnard-Lorig, C., Colon-Carmona, A., Bauch, M., Hodge, S., Doerner, P., Bancharel, E., Dumas, C., Haseloff, J., and Berger, F. (2001). Dynamic analyses of the expression of the histone::YFP fusion protein in *Arabidopsis* show that syncytial endosperm is divided in mitotic domains. Plant Cell **13,** 495–509.

Bracha-Drori, K., Shichrur, K., Katz, A., Oliva, M., Angelovici, R., Yalovsky, S., and Ohad, N. (2004). Detection of protein–protein interactions in plants using bimolecular fluorescence complementation. Plant J. **40,** 419–427.

Braselton, J.P., Wilkinson, M.J., and Clulow, S.A. (1996). Feulgen staining of intact plant tissues for confocal microscopy. Biotech. Histochem. **71,** 84–87.

Campbell, R.E., Tour, O., Palmer, A.E., Steinbach, P.A., Baird, G.S., Zacharias, D.A., and Tsien, R.Y. (2002). A monomeric red fluorescent protein. Proc. Natl. Acad. Sci. USA **99,** 7877–7882.

Canales, C., Bhatt, A.M., Scott, R., and Dickinson, H. (2002). EXS, a putative LRR receptor kinase, regulates male germline cell number and tapetal identity and promotes seed development in *Arabidopsis*. Curr. Biol. **12,** 1718–1727.

Chanvivattana, Y., Bishopp, A., Schubert, D., Stock, C., Moon, Y.H., Sung, Z.R., and Goodrich, J. (2004). Interaction of Polycomb-group proteins controlling flowering in *Arabidopsis*. Development **131,** 5263–5276.

Chaudhury, A.M., and Berger, F. (2001). Maternal control of seed development. Semin. Cell Dev. Biol. **12,** 381–386.

Chaudhury, A.M., Ming, L., Miller, C., Craig, S., Dennis, E.S., and Peacock, W.J. (1997). Fertilization-independent seed development in *Arabidopsis thaliana*. Proc. Natl. Acad. Sci. USA **94,** 4223–4228.

Christensen, C.A., King, E.J., Jordan, J.R., and Drews, G.N. (1997). Megagametogenesis in *Arabidopsis* wild type and the *Gf* mutant. Sex. Plant Reprod. **10,** 49–64.

Clough, S.J., and Bent, A.F. (1998). Floral dip: A simplified method for Agrobacterium-mediated transformation of *Arabidopsis thaliana*. Plant J. **16,** 735–743.

Debeaujon, I., Léon-Kloosterziel, K.M., and Koorneef, M. (2000). Influence of the testa on seed dormancy, germination and longevity in Arabidopsis. Plant Physiol. **122,** 403–413.

Debeaujon, I., Nesi, N., Perez, P., Devic, M., Grandjean, O., Caboche, M., and Lepiniec, L. (2003). Proanthocyanidin-accumulating cells in *Arabidopsis* testa: Regulation of differentiation and role in seed development. Plant Cell **15,** 2514–2531.

Drews, G.N., and Yadegari, R. (2002). Development and function of the angiosperm female gametophyte. Annu. Rev. Genet. **36,** 99–124.

Ebel, C., Mariconti, L., and Gruissem, W. (2004). Plant retinoblastoma homologues control nuclear proliferation in the female gametophyte. Nature **429,** 776–780.

Elliot, R.C., Betzner, A.S., Huttner, E., Oakes, M.P., Tucker, W.Q.J., Gerentes, D., Perez, P., and Smyth, D.R. (1996). *AINTEGUMENTA*, an *APETALA2*-like gene of *Arabidopsis* with pleiotropic roles in ovule development and floral organ growth. Plant Cell **8,** 155–168.

Garcia, D., Fitz Gerald, J.N., and Berger, F. (2005). Maternal control of integument cell elongation and zygotic control of endosperm growth are coordinated to determine seed size in *Arabidopsis*. Plant Cell **17,** 52–60.

Garcia, D., Saingery, V., Chambrier, P., Mayer, U., Jürgens, G., and Berger, F. (2003). Arabidopsis *haiku* mutants reveal new controls of seed size by endosperm. Plant Physiol. **131,** 1661–1670.

Grossniklaus, U., Vielle-Calzada, J.-P., Hoeppner, M.A., and Gagliano, W.B. (1998). Maternal control of embryogenesis by *MEDEA*, a polycomb group gene in *Arabidopsis*. Science **280,** 446–450.

Guitton, A.E., and Berger, F. (2005). Loss-of-function of *MULTICOPY SUPPRESSOR OF IRA 1* produces non-viable parthenogenetic embryos in *Arabidopsis*. Curr. Biol. **15,** 750–754.

Guitton, A.E., Page, D.R., Chambrier, P., Lionnet, C., Faure, J.E., Grossniklaus, U., and Berger, F. (2004). Identification of new members of Fertilisation Independent Seed polycomb group pathway involved in the control of seed development in *Arabidopsis thaliana*. Development **131,** 2971–2981.

Haseloff, J. (1999). GFP variants for multispectral imaging of living cells. Methods Cell Biol. **58,** 139–151.

Haughn, G., and Chaudhury, A. (2005). Genetic analysis of seed coat development in *Arabidopsis*. Trends Plant Sci. **10,** 472–477.

Ingouff, M., Haseloff, J., and Berger, F. (2005). Polycomb group genes control developmental timing of endosperm. Plant J. **42,** 663–674.

Inze, D. (2005). Green light for the cell cycle. EMBO J. **24,** 657–662.

Johnson, C.S., Kolevski, B., and Smyth, D.R. (2002). *TRANSPARENT TESTA GLABRA2*, a trichome and seed coat development gene of *Arabidopsis*, encodes a WRKY transcription factor. Plant Cell **14,** 1359–1375.

Kasahara, R.D., Portereiko, M.F., Sandaklie-Nikolova, L., Rabiger, D.S., and Drews, G.N. (2005). MYB98 is required for pollen tube guidance and synergid cell differentiation in *Arabidopsis*. Plant Cell **17,** 2981–2992.

Klucher, K.M., Chow, H., Reiser, L., and Fischer, R.L. (1996). The *AINTEGUMENTA* gene of *Arabidopsis* required for ovule and female gametophyte development is related to the floral homeotic gene *APETALA2*. Plant Cell **8,** 137–153.

Köhler, C., Hennig, L., Bouveret, R., Gheyselinck, J., Grossniklaus, U., and Gruissem, W. (2003). *Arabidopsis* MSI1 is a component of the MEA/FIE polycomb group complex and required for seed development. EMBO J. **22,** 4804–4814.

Luo, M., Bilodeau, P., Dennis, E.S., Peacock, W.J., and Chaudhury, A. (2000). Expression and parent-of-origin effects for *FIS2*, *MEA*, and *FIE* in the endosperm and embryo of developing *Arabidopsis* seeds. Proc. Natl. Acad. Sci. USA **97,** 10637–10642.

Luo, M., Dennis, E.S., Berger, F., Peacock, W.J., and Chaudhury, A. (2005). *MINISEED3* (*MINI3*), a WRKY family gene, and *HAIKU2* (*IKU2*), a leucine-rich repeat (LRR) kinase gene, are regulators of seed size in *Arabidopsis*. Proc. Natl. Acad. Sci. USA **102,** 17531–17536.

Mosquna, A., Katz, A., Shochat, S., Grafi, G., and Ohad, N. (2004). Interaction of FIE, a polycomb protein, with pRb: A possible mechanism regulating endosperm development. Mol. Genet. Genomics **271,** 651–657.

Nowack, M.K., Grini, P.E., Jakoby, M.J., Lafos, M., Koncz, C., and Schnittger, A. (2006). A positive signal from the fertilization of the egg cell sets off endosperm proliferation in angiosperm embryogenesis. Nat. Genet. **38,** 63–67.

Ohad, N., Yadegari, R., Margossian, L., Hannon, M., Michaeli, D., Harada, J.J., Goldberg, R.B., and Fischer, R.L. (1999). Mutations in *FIE*, a WD polycomb group gene, allow endosperm development without fertilization. Plant Cell **11,** 407–416.

Reiser, L., Modrusan, Z., Margossian, L., Samach, A., Ohad, N., Haughn, G.W., and Fischer, R.L. (1995). The *BELL1* gene encodes a homeodomain protein involved in pattern formation in the *Arabidopsis* ovule primordium. Cell **83,** 735–742.

Schiefthaler, U., Balasubramanian, S., Sieber, P., Chevalier, D., Wisman, E., and Schneitz, K. (1999). Molecular analysis of NOZZLE, a gene involved in pattern formation and early sporogenesis during sex organ development in *Arabidopsis thaliana*. Proc. Natl. Acad. Sci. USA **96,** 11664–11669.

Schneitz, K., Hulskamp, M., Kopczak, S.D., and Pruitt, R.E. (1997). Dissection of sexual organ ontogenesis: A genetic analysis of ovule development in *Arabidopsis thaliana*. Development **124,** 1367–1376.

Schnittger, A., Schöbinger, U., Stierhof, Y.D., and Hülskamp, M. (2002). Ectopic B-type cyclin expression induces mitotic cycles in endoreduplicating *Arabidopsis* trichomes. Curr. Biol. **12,** 415–420.

Schruff, M.C., Spielman, M., Tiwari, S., Adams, S., Fenby, N., and Scott, R.J. (2006). The *AUXIN RESPONSE FACTOR 2* gene of *Arabidopsis* links auxin signalling, cell division, and the size of seeds and other organs. Development **133,** 251–261.

Weijers, D., Van Hamburg, J.P., Van Rijn, E., Hooykaas, P.J., and Offringa, R. (2003). Diphtheria toxin-mediated cell ablation reveals interregional communication during Arabidopsis seed development. Plant Physiol. **133,** 1882–1892.

Wildwater, M., Campilho, A., Perez-Perez, J.M., Heidstra, R., Blilou, I., Korthout, H., Chatterjee, J., Mariconti, L., Gruissem, W., and Scheres, B. (2005). The *RETINOBLASTOMA-RELATED* gene regulates stem cell maintenance in *Arabidopsis* roots. Cell **123,** 1337–1349.

Yadegari, R., and Drews, G.N. (2004). Female gametophyte development. Plant Cell **16** (suppl.), S133–S141.

Yang, W.C., Ye, D., Xu, J., and Sundaresan, V. (1999). The *SPOROCYTELESS* gene of Arabidopsis is required for initiation of sporogenesis and encodes a novel nuclear protein. Genes Dev. **13,** 2108–2117.